

THREE DIMENSIONAL RE-MESHING FOR REAL TIME MODELING OF ADVANCING PROCESS IN MECHANIZED TUNNELING

Abdullah ALSAHLI, Janosch STASCHEIT and Günther MESCHKE

Institute for Structural Mechanics
Ruhr University Bochum
Universitätsstr. 150, Bochum 44801, Germany
e-mail: {abdullah.alsahly; janosch.stascheit; guenther.meschke}@rub.de
webpage: <http://www.sd.rub.de>

Key words: Adaptive Modeling, Steering algorithm, hybrid re-meshing, mechanized tunneling

Abstract. The simulation of the advancing process for arbitrary alignments during shield tunneling requires a continuous adaption of the finite element mesh in the vicinity of the tunnel face in conjunction with a steering algorithm for the Tunnel Boring Machine (TBM) advance. Moreover, the finite element mesh should match the actual motion path of the shield machine resulting from the FE-analysis in each excavation step. For this purpose, a technique to automatize the process of mesh generation based on hybrid mesh approach is proposed in which a new computational mesh in the vicinity of the tunnel face will be automatically generated within the advancing process. This contribution is concerned with the 3D automatic mesh generation of finite element models for numerical simulations of shield driven tunneling processes.

1 INTRODUCTION

In numerical simulations of shield driven tunneling processes, the realistic modeling of both the excavation process and the advancement of the Tunnel Boring Machine (TBM) is a challenge. For a better understanding of these processes during tunnel construction, the interactions between the shield machine and the surrounding soil need to be investigated, yet this excavation process is difficult to model with existing finite element models. In addition, the simulation of the advancement of the machine as an independent body which interacts with all relevant component of the model, requires a realistic kinematics model of the shield machine which is generally not included in computational models for TBM tunneling [14]. A prototype for a process-oriented three-dimensional finite element model for simulations of shield-driven tunnels in soft, water-saturated soil has been developed and successfully used for systematic numerical studies of interactions in mechanized

tunneling [7], which has been re-formulated and extended to partially saturated soils and more advanced constitutive models for soils in the context of a integrated design support system for mechanized tunneling (see, e.g. [11, 10]). Furthermore, several finite element models have been proposed, addressing the difficulties inherent in the simulation of the excavation process. Many of these models account for excavation by removing finite elements from the excavated volume in front of the machine, and then by applying the nodal forces necessary to preserve equilibrium [1, 3]. A more realistic representation of the excavation process, based on mesh adaptation, using so-called "excavating elements" in front of the machine has been proposed by [8]. In this paper, a steering algorithm and re-meshing strategy are presented in the context of 3D modeling TBM advancement processes. The algorithm serves as an virtual guidance system which automatically determines the exact position and the driving direction of the TBM in three dimensional space. A new approach for hybrid mesh generation is proposed, which adapts the spatial discretization in the vicinity of the tunnel face according to the actual position of the TBM. This hybrid mesh attempts to combine full advantage of the numerical accuracy and practical aspects of structured hexahedra meshes, while the numerical error can be controlled by the chosen density and interpolation order of the unstructured tetrahedral mesh within the excavation region denoted as region of interest.

2 FINITE ELEMENT MODELING OF ADVANCEMENT PROCESSES

2.1 The kinematic model of the shield machine

A close to reality modeling of the advancing process and the interaction between the TBM and the surrounding environment requires a realistic kinematic model of the shield machine [4]. Therefore, a nonlinear kinematic analysis of the shield, based on the action forces imposed on the shield and on the inertial forces due to the shield, is performed. The action forces result from hydraulic jacks pushing against the machine, earth/slurry pressure at the cutting face, friction with surrounding soils, and the fluid flow of processes of the support fluid and grouting mortar, whereas the inertial forces are due to the self weight of the shield and of the equipment. Furthermore, the taper and the thickness of the shield skin are accounted for in the geometrical representation of the TBM (see figure 1), allowing for a realistic distribution of the ground reaction forces in both circumferential and longitudinal directions. A Lagrangian finite element analysis of large deformations that satisfies both the displacements and forces boundary conditions imposed by shield machine operation provides the actual TBM kinematics. Within this approach the shield machine is modeled as a deformable body using a Total Lagrangian Finite Element formulation.

2.2 Steering correction algorithm

The TBM is advanced by hydraulic jacks that are attached to the machine which push against the previously installed lining ring. The pressure exerted by these jacks must

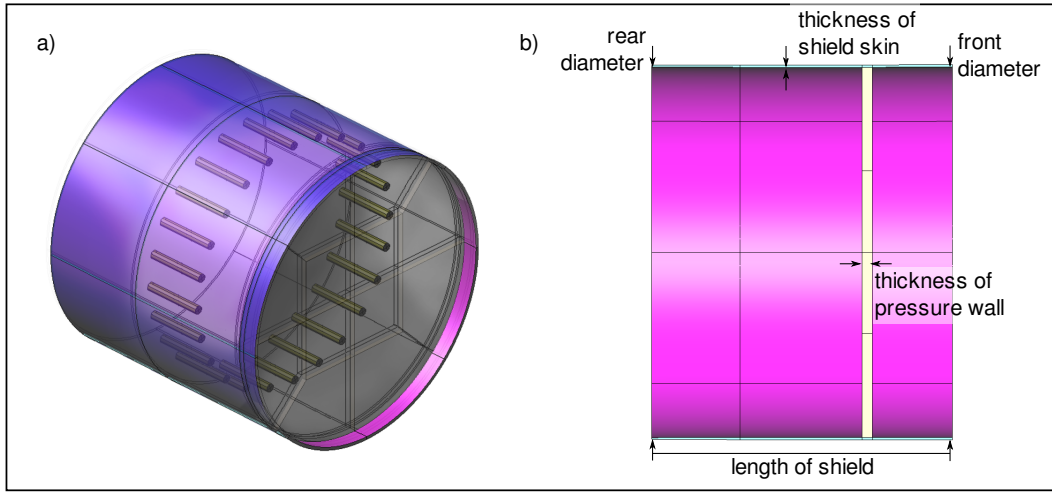


Figure 1: Geometrical model of the shield machine: a) transparent view of shield geometry and hydraulic jacks; b) dimensions of the shield

overcome the resistance generated by the surrounding soil. Moreover, since the machine is heavier at the head, the jack forces are highest in the invert and conversely the lowest in the crown. Driving the shield along curves requires additional steering forces along the sides to ensure the machine follows the intended three dimensional curve. When the steering or the so-called deviation correction is needed, the pressure at individual hydraulic jacks is adjusted to produce deflection torques in the horizontal and vertical direction. In the computational model, the shield machine is pushed forward by extending hydraulic jacks represented by CRISFIELD truss elements. These are connected to both the surface of the lining and the shield. The jack elongations are accomplished by providing initial strains which describe the desired elongation. Respective values for the jack pressures are obtained as a simulation result [13]. In accordance with tunneling practice, a reliable steering algorithm that provides the numerical model with the required information to keep the TBM on the track is developed. This TBM advancement algorithm serves as an artificial guidance system which automatically determines the exact position and the driving direction of the TBM in three dimensional space providing the vertical and horizontal deviation, shield orientation and direct input for the jacking cylinders. For this purpose, the steering algorithm provides a non-uniform jack thrusts, forcing the reference point on the shield to a given point along the alignment. The method for which the machine is advanced is as follows:

1. The geometry of the tunnel path is described by a set of coordinates in three dimensional space.
2. Each jack element J^i is defined by its end points: its connection to the lining \mathbf{p}_L and its connection to the shield wall \mathbf{p}_S as shown in figure 2.

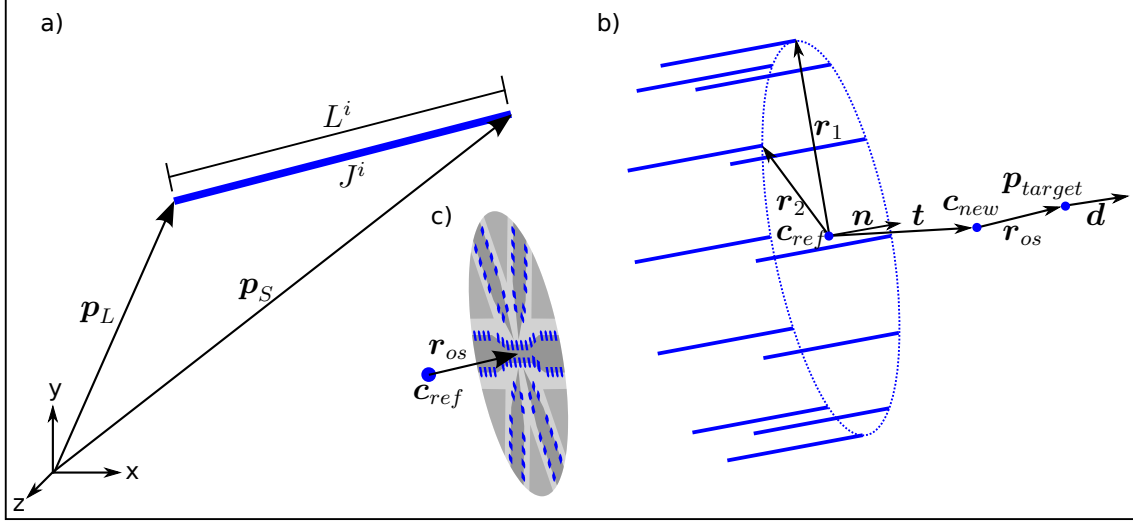


Figure 2: Definitions in the steering algorithm: a) measures related to one jack element J^i ; b) measures related to the steering algorithm; c) definition of the offset vector \mathbf{r}_{os}

3. A reference point \mathbf{c}_{ref} on the shield wall is specified to control the deviation of the machine from the intended path after each advancing step. This point is the centre of a circle formed by the tips of all n_J hydraulic jack elements on the shield end:

$$\mathbf{c}_{ref} = \frac{1}{n_J} \sum_i^{n_J} \mathbf{p}_S^i \quad (1)$$

Since this reference position differs from the centre of the cutting wheel, an offset vector \mathbf{r}_{os} is defined that points from the reference point to the centre of the cutting wheel.

4. The new position \mathbf{p}_{target} of the centre of the cutting wheel as well as a director \mathbf{d} for the heading of the shield are required for advancing the shield. These are determined from the chainage of the tunnel alignment. In the k^{th} alignment station \mathbf{a}^k , these quantities are obtained by:

$$\mathbf{p}_{target} = \mathbf{a}^{k+1} \quad (2)$$

$$\mathbf{d} = \frac{\mathbf{a}^{k+2} - \mathbf{a}^{k+1}}{\|\mathbf{a}^{k+2} - \mathbf{a}^{k+1}\|} \quad (3)$$

In combination with the offset vector, the new position of the reference point is obtained:

$$\mathbf{c}_{new} = \mathbf{p}_{target} - \mathbf{r}_{os} \quad (4)$$

From these positions, a translation vector \mathbf{t} , that defines the pure translation of the reference point from its current position to its target position, is calculated:

$$\mathbf{t} = \mathbf{c}_{new} - \mathbf{c}_{ref} \quad (5)$$

Subsequently, the current heading of the shield needs to be determined. For this purpose, two radial vectors \mathbf{r}_1 and \mathbf{r}_2 are defined, from which the current heading \mathbf{n} can be derived by:

$$\mathbf{n} = \frac{\mathbf{r}_1 \times \mathbf{r}_2}{\|\mathbf{r}_1 \times \mathbf{r}_2\|} \quad (6)$$

5. The new position $\mathbf{p}_{S,new}^i$ of each jack element after steering is computed using the a standard cartesian rotation matrix \mathbf{A}_{rot} in three dimensional space. The rotation axis is perpendicular to both \mathbf{n} and \mathbf{d} :

$$\mathbf{v} = \begin{cases} \mathbf{n} \times \mathbf{d}, & \text{if } \mathbf{n} \neq \mathbf{d} \\ \{1, 0, 0\} & \text{else.} \end{cases} \quad (7)$$

By this choice of a rotation axis, the rotation angle α and a respective rotation matrix \mathbf{A}_{rot} can be computed:

$$\begin{aligned} \alpha &= \arccos(\mathbf{n} \cdot \mathbf{d}) \\ \mathbf{A}_{rot} &= \begin{pmatrix} C + v_1^2(1-C) & v_1v_2(1-C) - v_3S & v_1v_3(1-C) + v_2S \\ v_2v_1(1-C) + v_3S & C + v_2^2(1-C) & v_2v_3(1-C) - v_1S \\ v_3v_1(1-C) - v_2S & v_3v_2(1-C) + v_1S & C + v_3^2(1-C) \end{pmatrix} \quad (8) \\ &\text{with } C = \cos \alpha \text{ and } S = \sin \alpha \end{aligned}$$

6. The new position of each jack on the shield wall is determined to obtain the required jack elongations:

$$\mathbf{p}_{S,new}^i = \mathbf{c}_{new} + \mathbf{A}_{rot}(\mathbf{p}_S - \mathbf{c}_{ref}) \quad (9)$$

7. The new reference length and the elongations are computed and applied as an internal Green Lagrange strain for each CRISFIELD truss element:

$$L_{new}^i = \|\mathbf{p}_{S,new} - \mathbf{p}_L\| \quad (10)$$

$$\mathbf{E}_{11} = \frac{L_{new}^2 - l_{ref}^2}{2l_{ref}^2} \quad (11)$$

3 AUTOMATIC MODELING OF THE EXCAVATION PROCESS

The simulation of the advancing process for arbitrary alignments by means of the proposed steering algorithm requires a continuous adaption of the finite element mesh in the vicinity of the tunnel face. Furthermore, the finite element mesh should match the actual motion path of the shield machine resulting from the FE-analysis in each excavation step. For this purpose, a re-meshing algorithm is developed in order to automate the process of mesh generation in a domain in the vicinity of the tunnel face within the advancing process.

3.1 Tunnel geometry

The two major representation schemes used to describe a solid model are Constructive Solid Geometry (CSG) schemes and Boundary Representations (B-Rep) schemes [6]. In an underground excavation the site geometry is often irregularly shaped, therefore, the B-rep scheme is seen to be the most efficient as it can easily describe the polyhedral surfaces needed to represent the tunnel geometry. A generalized cylinder is a representation of an elongated object that has a main axis (directrix or spine) and a smoothly varying cross section (generatrix) [9, 12]. A directrix and a generatrix can both be open or closed curves. In tunneling simulation, the directrix is a bounded 3D curve representing the tunnel path, and the generatrix is a closed curve representing the tunnel cross section. The 3D tunnel path and the tunnel cross section are approximated using piecewise linear line segments that are optimized to match the circular geometry of the TBM. The surface geometry of a tunnel is created by sweeping the 2D cross section polygon along the piecewise linear tunnel path, as this is a quite common approach in underground engineering structures.

3.2 The meshing algorithm

The main aim of this meshing algorithm is to describe the new geometry by generating a new mesh automatically. By using the so-called piecewise linear system (PLS), not only is the boundary of excavation path described but also the external boundary of the re-meshing domain. Figure 3 illustrates one possible representation of the excavation geometry by means of a piecewise liner system after one advancing step. The internal facet of the PLS should be automatically updated to describe the new internal boundary, where the external facets are still fixed.

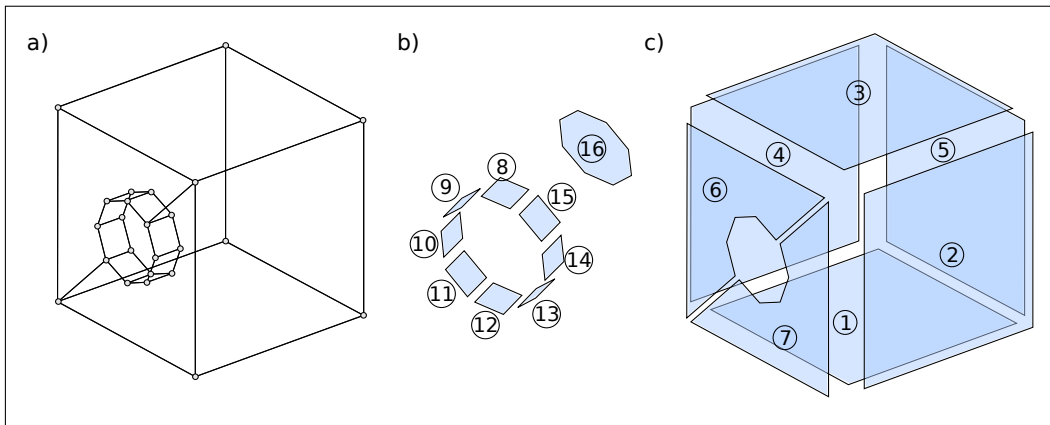


Figure 3: Representation of the excavation geometry by means of PLS: (a) Region of interest represented as PLS; (b) Internal boundary; (c) External boundary

This can be realized by sweeping the new facets representing the new excavated part and adding it to the PLS after each advancing step. The kinematic analysis of the shield

within the steering procedure provides the exact position and geometry of the new facets as well as the center of the cutting wheel and some reference points. To mesh the domain, a 3D Delaunay meshing algorithm TetGen [5] is used to generate an unstructured mesh consisting of tetrahedral elements. Delaunay-based algorithms are capable of producing quality meshes and provide control over mesh sizing throughout the domain. The major components of information required by the meshing algorithm are as follows:

- the input domain, which is a polyhedron, that defines the geometry of the problem,
- the position of the cutting head after each advancing step,
- a set of optional optimization criteria in order to control the quality of the mesh and the compatibility with neighboring domains.

3.3 Region of interest

Let V be a homogeneous and isotropic deformable body which occupies a domain $\Omega \subset \mathbf{R}^d (d = 2 \text{ or } 3)$ with a boundary $\Gamma \subset \mathbf{R}^{d-1}$. In this proposed re-meshing technique, the domain Ω of the complete simulation model is divided into 2 non-overlapping sub-domains Ω_1 and Ω_2 with $\Omega = \Omega_1 \cup \Omega_2$ and $\Omega_1 \cap \Omega_2 = \emptyset$. Each sub-domain Ω_i might represent either an excavation domain (named as region of interest) or the surrounding soil around this region with different layers of the geological formation. The boundary Γ_i of a sub-domain Ω_i can represent the interface between neighboring sub-domains or the internal boundary of the excavation domain. Here, the region of interest represented by Ω_1 is the region of the mesh that is continuously generated during TBM advance in the vicinity of the tunnel face. It must include at least the excavation geometry. It can be as large as the whole simulation domain or be limited to a small region around the heading face. In any case, the engineer will make the decision based on the available data and his engineering experience. In Figure 3 the boundary Γ_1 of the region of interest is represented by a closed polyhedron. To enable a dynamic and efficient simulation of arbitrary TBM advancement paths, information of the target excavation path is incorporated in the definition of the region of interest.

3.4 Hybrid mesh

The hybrid mesh approach attempts to combine the advantages of both structured and unstructured mesh layouts. The hexahedral elements are used in regions where no complex geometries exist, no re-meshing is required, and the numerical accuracy and practical aspects of structured hexahedra meshes are preserved. Whereas the tetrahedral elements are generated automatically describes the complex geometry (i.e. excavation boundary), while deficiency inherent to unstructured tetrahedral meshes is introduced only in the excavation region named region of interest.

To obtain a compatible hybrid mesh we should ensure a proper connectivity such that the internal tetrahedral elements (within the region of interest) are connected properly to

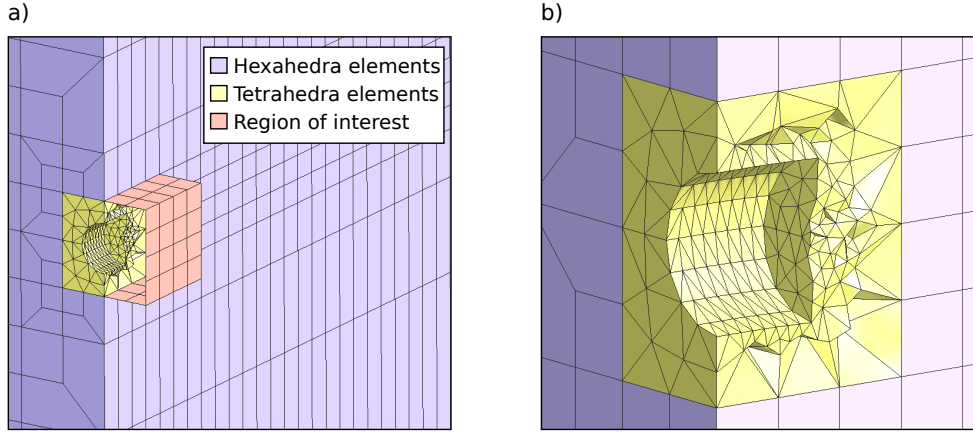


Figure 4: Hybrid mesh representation of excavation geometry; (a) Mesh components (b) Compatible mesh using hexahedral and tetrahedral elements.

the external hexahedral elements (at the boundary of the region of interest). Here, 27-noded quadratic hexahedral elements and 10-noded quadratic tetrahedral elements are employed. In other words, the resultant triangular surface mesh of the tetrahedral elements match exactly the quadrilateral surface mesh of the hexahedral elements surrounding the region of interest. The resulting mesh of this hybrid approach will automatically match both the external boundary in terms of connectivity to an existing boundary mesh and, internally, the projected motion path of the shield and the heading face as shown in Figure 4.

3.5 Modeling of excavation

The re-meshing algorithm works in conjunction with the steering algorithm. The steering algorithm simulates the advancing process in a step-by-step procedure. After each advancing step the re-meshing algorithm is invoked and generates a new computational mesh describing the new excavation geometry. The re-meshing algorithm uses the results from the steering algorithm as input for generating the new mesh. The exact geometry and position of the TBM after each advancing step will be extracted and used to generate the new mesh preserving the deformed configuration of the previous excavated geometry. By doing so, the excavation and the advancement of the shield machine are numerically simulated in a continuous manner. After obtaining the new mesh, several mesh operations and optimization techniques are required as follows:

- Optimization algorithm to project all central nodes of the higher order tetrahedral elements to their correct position in order to represent the exact curve and the circular shape of the shield.
- Generation of a new surface mesh to represent the excavation boundary, tunnel face

and contact surfaces.

- Variable transfer algorithm: after the re-meshing, the values of the stresses and the internal variables on the new mesh need to be calculated from those obtained in the original deformed mesh. This is necessary because the equilibrium condition needs to be satisfied before conducting the next advancing step. An appropriate algorithm based on Superconvergent Patch Recovery (SPR) [2] for the transfer of these internal variables is adopted.

4 APPLICATION EXAMPLES

In this section, two examples are presented to demonstrate the flexibility of the re-meshing algorithm and the applicability for driving the machine along curved alignment. In the first example, the re-meshing algorithm is invoked to generate a proper mesh describes the geometry of the of the excavated path. Within this example the mesh will be regenerated automatically after each advancing step. Furthermore, the machine is to be advanced in the soil following an arbitrary path. The geometry of the excavation path is defined by means of the following parameters:

- The radius of the excavation (radius of the machine) = $5.25m$.
- The number of the segments on the circular geometry of the machine = 20.
- The size of the advancing step is = $0.5m$ in each step.
- The tunnelling path is assumed as a quadratic path described by means of a sequence of points.

After each advancing step the original mesh is replaced with a new mesh to represent the complete excavation path. The goal of this example is only to show that the new generated mesh conforms to the excavation geometry at the end of each advancing step. The generated meshes after different advancing steps are shown in 5 . The advancing is performed in x-direction whereas the steering is performed in each advancing step in the two other directions y and z simultaneously. Cross sections through the excavation path are visualized where the x-y plane and y-z plane are considered.

In this second example, the advancing process and the application of the new excavation technique are demonstrated by considering the southwestern part of the L9 tunnel "Mas Blau". It consists of a single twin-track tunnel that runs along a strongly curved path. The tunnel is characterized by a diameter (D) of 9.4 m and a cover depth of 14.0 m. The tunnel alignment and the simulation domain are shown in Figure 6. In this study, the elastic model for the lining and the shield machine with basic material properties summarized in Table 1 is adopted. For the modeling of the soil, a DRUCKER-PRAGER plasticity model is used.

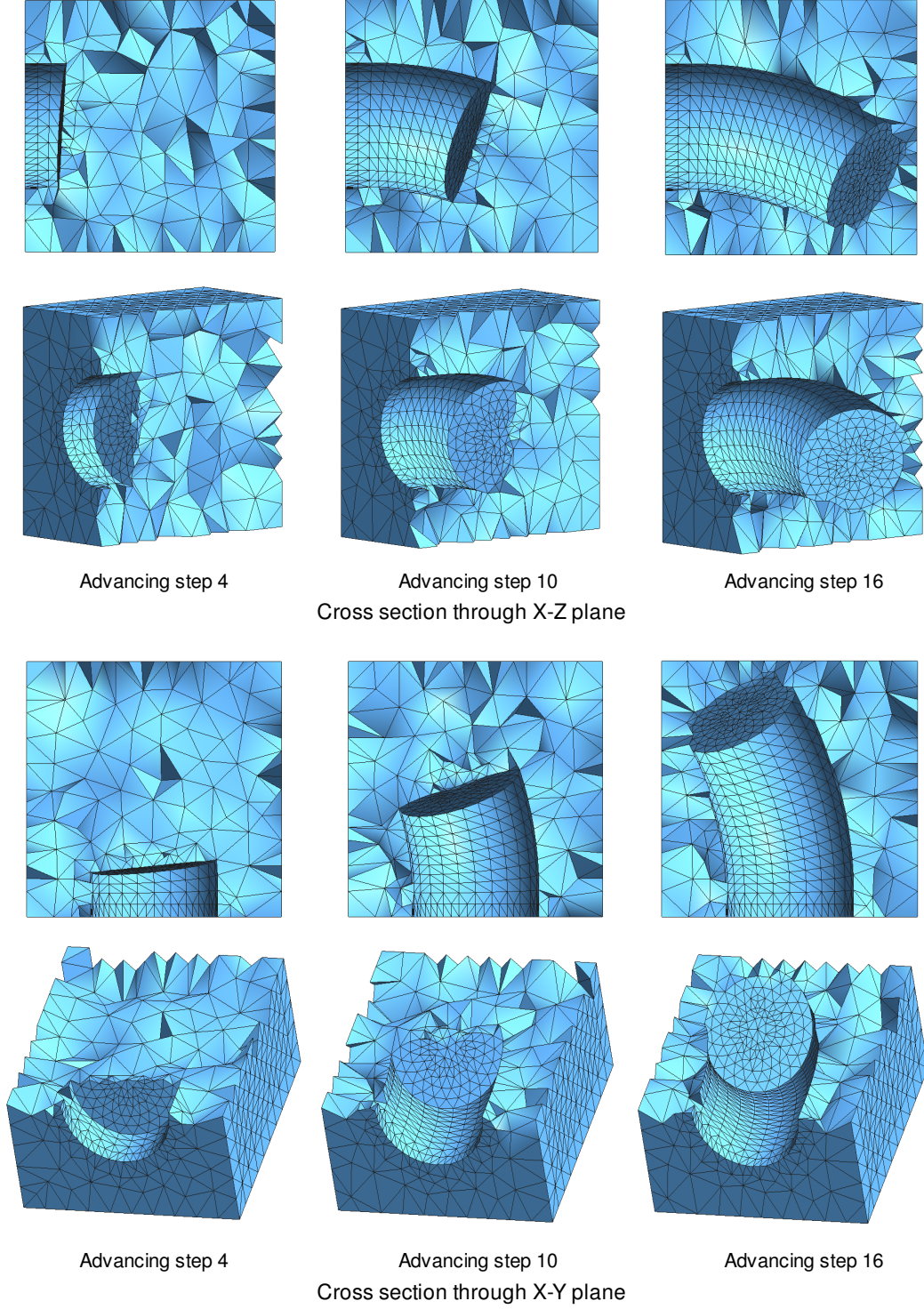


Figure 5: Conformal tetrahedral mesh for the steering of the TBM, different cross-sections through the excavation path in x-y plane and y-z plane.

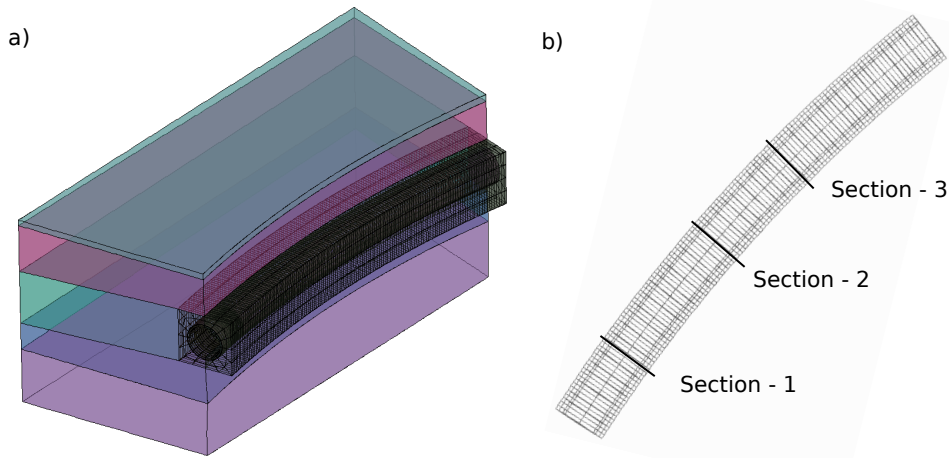


Figure 6: L9 Tunnel "Mas Blau" ; (a) representation of the simulation domain (b) tunnel alignment and the position of three cross section

Table 1: Material parameters used in the finite element model

model part	γ [kN/m ³]	φ [°]	c [MPa]	E [MPa]	ν [-]
Lining	25.0	-	-	30000	0.2
Shield	76.2	-	-	210000	0.27
Soil	28.5	29	0.11	2100	0.28

Figure 7 shows the obtained jack forces in three different positions during the simulation of the advancing process. The nonuniform jack thrust distributions illustrate the power of the steering algorithm in conjunction with the developed re-meshing algorithm and the efficiency of the algorithm that controls the TBM position and keeps it on the intended target alignment. The diagram in Figure 7 shows the change of the steering forces during the steering process in the horizontal and vertical directions. Thus, the finite element results are consistent with the actual shield advancement procedure and guidance system.

The results of the re-meshing algorithm are illustrated in Figure 8 for different advancing steps. The results obtained from this simulation demonstrate the efficiency and the high applicability of the re-meshing algorithm to capture the exact excavation path. In addition, it is possible to advance the TBM at different speed and the meshing algorithm will account for the size of the mesh automatically. In standard numerical analyses of TBM advance, where the mesh is generated a priori, this would not be possible.

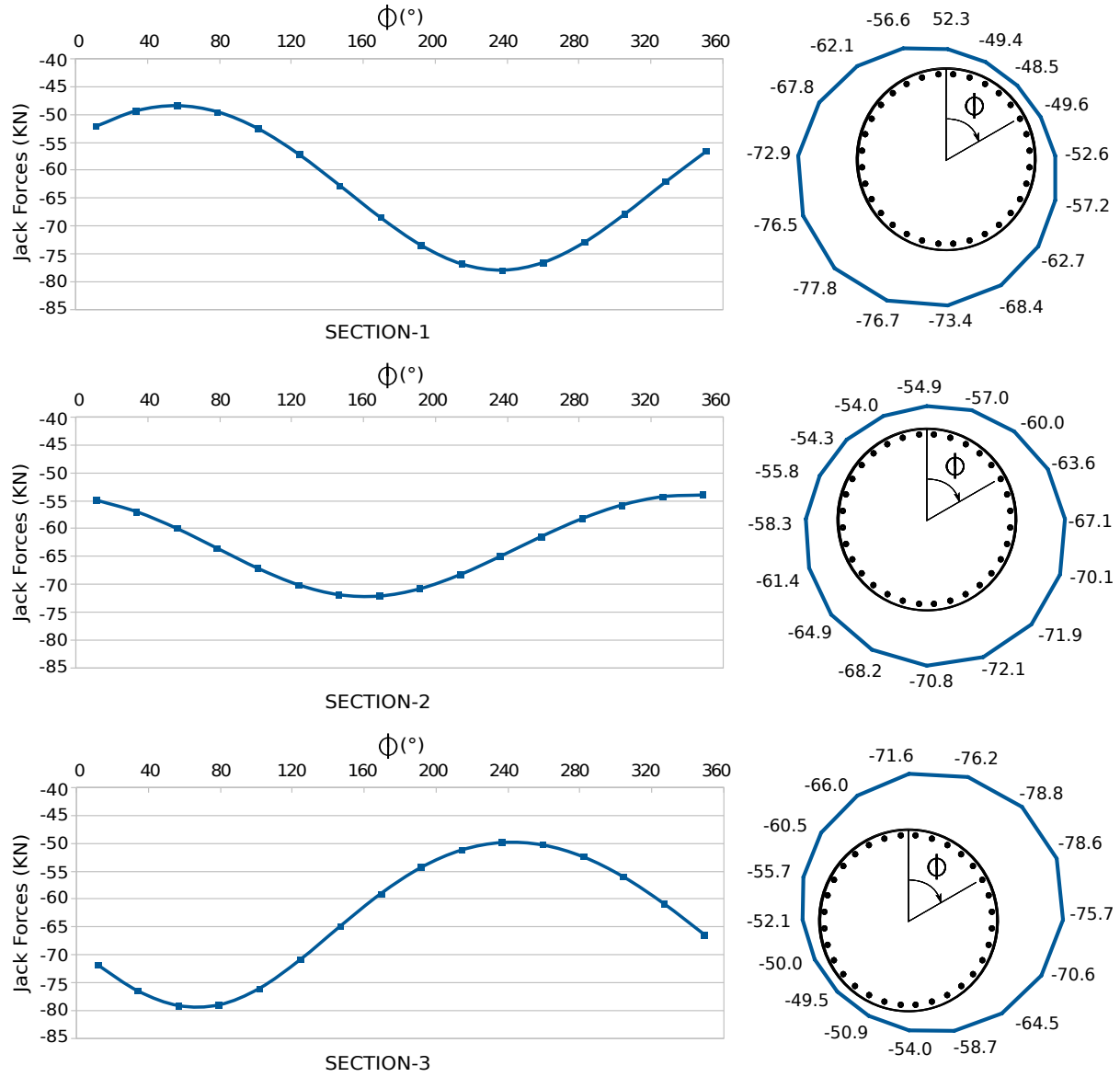


Figure 7: Distribution of the Hydraulic jack forces along the shield wall in different advancing steps (Section-1, Section-2, Section-3 in Figure 6)

5 CONCLUSIONS

A fully automatic re-meshing technique for the modeling of the advancement and the excavation process of shield tunneling has been proposed, with an efficient and automatic algorithm to simulate the advancing process along arbitrary tunnel alignments. The kinematic shield model was used to simulate the advancing process along curved tunnel alignment. The advancement process of the TBM and the soil excavation was simulated step wise using a new steering and a problem specific re-meshing algorithm. The steering

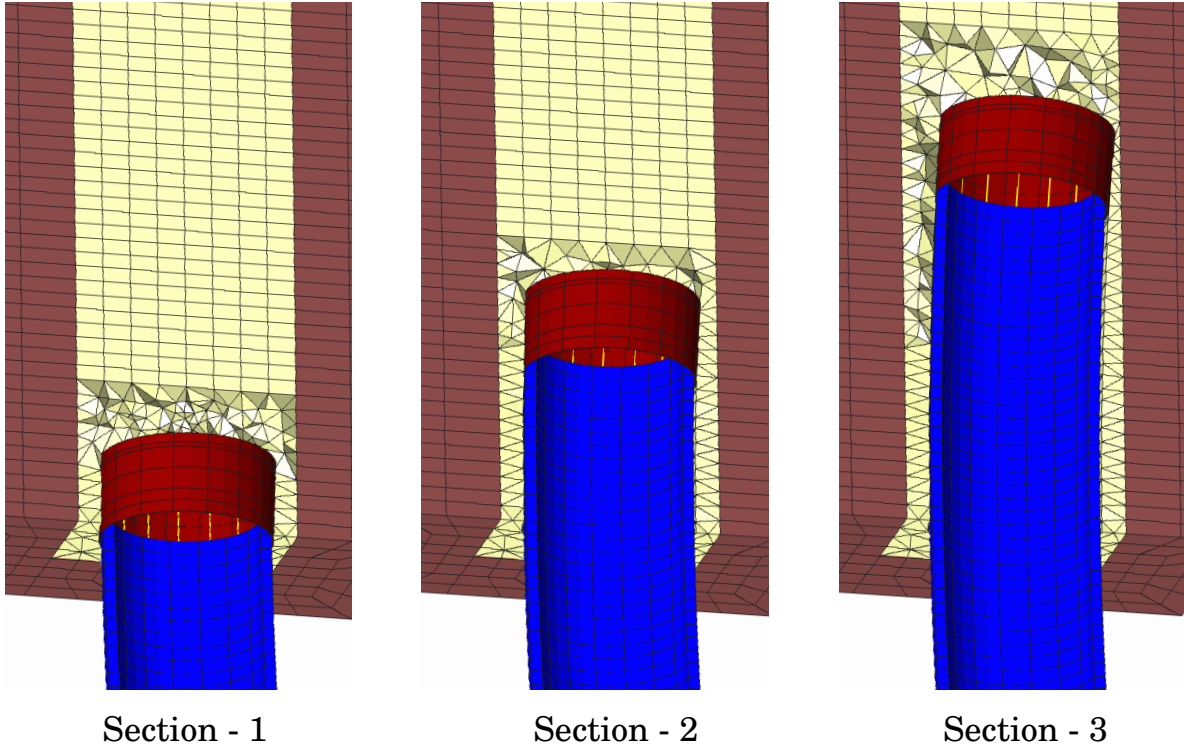


Figure 8: FE mesh representing the excavation geometry for different advancing steps (Section-1, Section-2, Section-3 in Figure 6)

algorithm in conjunction with the re-meshing algorithm are independent from any a priori generated discretization and consider the ground movement around the shield. It was shown, that the proposed computational model is able to simulate the actual motion of the TBM along arbitrary paths with minimum effort required in the preprocessing stage. Further developments of the model will focus on the influence of the discretization error during the excavation process.

6 ACKNOWLEDGEMENTS

Financial support was provided by the German Science Foundation (DFG) in the framework of project C1 of the Collaborative Research Center SFB 837 "Interaction Modeling in Mechanized Tunneling". This support is gratefully acknowledged.

REFERENCES

- [1] S. Bernat and B. Cambou. Soil - structure interaction in shield tunnelling in soft soil. *Computers and Geotechnics*, 22(3/4):221–242, 1998.
- [2] B. Boroomand and O. Zienkiewicz. Recovery by equilibrium in patches (rep). *International journal for numerical methods in engineering*, 40(1):137–164, 1997.

- [3] G. Clough, B. Sweeney, and R. Finno. Measured soil response to epb shield tunneling. *Journal of Geotechnical Engineering*, 109(2):131–149, 1983.
- [4] R. Finno and G. Clough. Evaluation of soil response to EPB shield tunneling. *Journal of Geotechnical Engineering*, 111(2):155–173, 1985.
- [5] S. Hang. Tetgen. *A quality tetrahedral mesh generator and three-dimensional Delaunay triangulator. Version, 1*, 2007.
- [6] C. M. Hoffmann. *Geometric and solid modeling: an introduction*. Morgan Kaufmann Publishers Inc., 1989.
- [7] T. Kasper and G. Meschke. A 3D finite element model for TBM tunneling in soft ground. *International Journal for Numerical and Analytical Methods in Geomechanics*, 28:1441–1460, 2004.
- [8] K. Komiya, K. Soga, H. Akagi, T. Hagiwara, and M. Bolton. Finite element modelling of excavation and advancement processes of a shield tunnelling machine. *Soils and Foundations*, 39(3):37–52, 1999.
- [9] T. Maekawa, N. M. Patrikalakis, T. Sakkalis, and G. Yu. Analysis and applications of pipe surfaces. *Computer Aided Geometric Design*, 15(5):437–458, 1998.
- [10] G. Meschke, F. Nagel, and J. Stascheit. Computational simulation of mechanized tunneling as part of an integrated decision support platform. *Journal of Geomechanics (ASCE)*, 11(6):519–528, 2011. Special Issue: Material and Computer Modeling.
- [11] F. Nagel, J. Stascheit, and G. Meschke. Numerical simulation of interactions between the shield supported tunnel construction process and the response of soft, water saturated soils. *International Journal of Geomechanics (ASCE)*, 12(6):689–696, 2011.
- [12] J. Pegna. *Variable sweep geometric modeling*. PhD thesis, Stanford University, 1987.
- [13] J. Stascheit. *Parallelisation and model generation methods for large-scale simulations of shield tunnelling processes*. PhD thesis, Ruhr-Universität Bochum, 2010.
- [14] M. Sugimoto and A. Sramoon. Theoretical model of shield behaviour during excavation. I: Theory. *Journal of Geotechnical and Geoenvironmental Engineering*, 128(2):138–155, 2002.